



Published in final edited form as:

*Heart Rhythm*. 2008 December ; 5(12): 1726–1734. doi:10.1016/j.hrthm.2008.09.008.

## Role of late sodium current in modulating the proarrhythmic and antiarrhythmic effects of quinidine

**Lin Wu, MD,**

From Pharmacological Sciences, CV Therapeutics, Inc., Palo Alto, California

**Donglin Guo, MD, PhD,**

Main Line Health Heart Center, Wynnewood, Pennsylvania

**Hong Li, MS,**

From Pharmacological Sciences, CV Therapeutics, Inc., Palo Alto, California

**James Hackett, PhD,**

Hackett and Associates, Inc., San Jose, California

**Gan-Xin Yan, MD, PhD,**

Main Line Health Heart Center, Wynnewood, Pennsylvania

**Zhen Jiao, MD,**

Main Line Health Heart Center, Wynnewood, Pennsylvania

**Charles Antzelevitch, PhD, FHRS,**

Masonic Medical Research Laboratory, Utica, New York

**John C. Shryock, PhD, and**

From Pharmacological Sciences, CV Therapeutics, Inc., Palo Alto, California

**Luiz Belardinelli, MD**

From Pharmacological Sciences, CV Therapeutics, Inc., Palo Alto, California

### Abstract

**BACKGROUND**—Quinidine is used to treat atrial fibrillation and ventricular arrhythmias. However, at low concentrations, it can induce torsade de pointes (TdP).

**OBJECTIVE**—The purpose of this study was to examine the role of late sodium current ( $I_{Na}$ ) as a modulator of the arrhythmogenicity of quinidine in female rabbit isolated hearts and cardiomyocytes.

**METHODS**—Epicardial and endocardial monophasic action potentials (MAPs), ECG signals, and ion channel currents were measured. The sea anemone toxin ATX-II was used to increase late  $I_{Na}$ .

**RESULTS**—Quinidine had concentration-dependent and often biphasic effects on measures of arrhythmogenicity. Quinidine increased the duration of epicardial MAP ( $MAPD_{90}$ ), QT interval, transmural dispersion of repolarization (TDR), and ventricular effective refractory period. Beat-to-beat variability of  $MAPD_{90}$  (BVR), the interval from peak to end of the T wave ( $T_{peak-Tend}$ ) and index of  $T_{peak-Tend}/QT$  interval were greater at 0.1 to 3  $\mu\text{mol/L}$  than at 10–30  $\mu\text{mol/L}$  quinidine. In the presence of 1 nmol/L ATX-II, quinidine caused significantly greater concentration-dependent and biphasic changes of  $T_{peak-Tend}$ , TDR, BVR, and index of  $T_{peak-Tend}/QT$

interval. Quinidine (1  $\mu\text{mol/L}$ ) induced TdP in 2 and 13 of 14 hearts in the absence and presence of ATX-II, respectively. Increases of BVR, index of T<sub>peak</sub>-T<sub>end</sub>/QT interval, and T<sub>peak</sub>-T<sub>end</sub> were associated with quinidine-induced TdP. Quinidine inhibited I<sub>Kr</sub>, peak I<sub>Na</sub>, and late I<sub>Na</sub> with IC<sub>50</sub>s of  $4.5 \pm 0.3 \mu\text{mol/L}$ ,  $11.0 \pm 0.7 \mu\text{mol/L}$ , and  $12.0 \pm 0.7 \mu\text{mol/L}$ .

**CONCLUSION**—Quinidine had biphasic proarrhythmic effects in the presence of ATX-II, suggesting that late I<sub>Na</sub> is a modulator of the arrhythmogenicity of quinidine. Enhancement of late I<sub>Na</sub> increased proarrhythmia caused by low but not high concentrations of quinidine.

### Keywords

Quinidine; Late sodium current; Torsade de pointes; Arrhythmia mechanism; Action potential duration; Ion channels; Membrane potential; QT interval

## Introduction

Quinidine is a class IA antiarrhythmic drug with the effect of reducing multiple ion currents, including both Na<sup>+</sup> and K<sup>+</sup> channel currents (e.g., I<sub>Na</sub>, I<sub>Kr</sub>, I<sub>Ks</sub>, I<sub>K1</sub>, I<sub>K-ATP</sub>, I<sub>to</sub>).<sup>1-3</sup> Quinidine is used to treat both atrial and ventricular tachyarrhythmias. By virtue of its electrophysiologic actions of inhibiting I<sub>K</sub> and increasing the ventricular effective refractory period, quinidine can also reduce arrhythmic activity in patients with short QT syndrome caused by gain of function of potassium channels<sup>3-4</sup> and in patients with Brugada syndrome caused by loss-of-function sodium channelopathies.<sup>3-6</sup> However, it has been recognized for decades that clinical use of quinidine is associated with recurrent syncope (i.e., quinidine syncope) and sudden death due to QT prolongation and polymorphic ventricular tachycardia (torsade de pointes [TdP]).<sup>1-2</sup> The incidence of TdP caused by quinidine is 1.5% to 8.8% or higher per patient-year of treatment.<sup>1-7</sup> Because the incidence of TdP is dose independent and the sensitivity of patients to the proarrhythmic effects of quinidine is highly variable,<sup>1</sup> an understanding of the causes of proarrhythmic effects of quinidine in patients has been difficult to achieve.

In cardiac tissue, quinidine produces an open-state block of the sodium channel, decreases the upstroke velocity of the action potential, and causes a use-dependent increase in the QRS interval. It also blocks I<sub>Kr</sub> and prolongs action potential duration (APD), an effect that is greater at slower than at faster heart rates.<sup>8</sup> Both Na<sup>+</sup> and K<sup>+</sup> channel block caused by a multi-ion-channel blocker are concentration dependent and can be potential mechanisms of either anti-arrhythmic or proarrhythmic activity.<sup>9</sup> Therefore, it has been difficult to clarify the mechanisms that are responsible for the proarrhythmic activity of quinidine. We hypothesized that if block of I<sub>Kr</sub> by quinidine reduced repolarization reserve more than block of I<sub>Na</sub> increased it, the drug would be proarrhythmic. This situation is likely to exist when repolarization reserve is decreased due to an enhancement of late I<sub>Na</sub>. Because repolarization reserve is reduced in the female rabbit heart treated with a low concentration of sea anemone toxin II (ATX-II) and exposure to ATX-II mimics the congenital or acquired conditions that increase late I<sub>Na</sub>, we investigated the proarrhythmic and antiarrhythmic effects of quinidine using this rabbit heart model. In addition, by taking advantage of the unusual biphasic quinidine-induced changes in electrophysiologic parameters and in the occurrence of TdP, it was possible in this study to analyze the probability of TdP as a function of increases in the values of a number of these individual parameters.

## Methods

Animal use conformed to the “Guide for the Care and Use of Laboratory Animals” published by the US National Institutes of Health (NIH Publication No. 85-23, revised 1996)

and was approved by the Institutional Animal Care and Use Committee of CV Therapeutics (Palo Alto, CA, USA). New Zealand white female rabbits (weight 2.5–3.5 kg) were sedated and then anesthetized using IM and IV xylazine and ketamine, respectively.

### Female rabbit isolated heart model

Rabbit hearts were excised and placed in a modified Krebs-Henseleit solution (pH 7.4, gassed with 95% O<sub>2</sub> and 5% CO<sub>2</sub>) of the following composition (in mmol/L): 118 NaCl, 2.8 KCl, 1.2 KH<sub>2</sub>PO<sub>4</sub>, 2.5 CaCl<sub>2</sub>, 0.5 MgSO<sub>4</sub>, 2.0 pyruvate, 5.5 glucose, 0.57 Na<sub>2</sub>EDTA, and 25 NaHCO<sub>3</sub>. The aorta was cannulated, and the heart was perfused at a rate of 20 mL/min with Krebs-Henseleit solution warmed to 37°C by the Langendorff method.<sup>9,10</sup> Complete AV block was induced by thermoablation of the AV nodal area, and hearts were paced at 1 Hz. A 10- to 20-minute period of equilibration was allowed before hearts were exposed to drugs.

### Monophasic action potential recording

Two pressure-contact Ag-AgCl monophasic action potential (MAP) electrodes were placed on the epicardium and endocardium at opposite sides of the left ventricle. Signals were digitized to determine the duration of the MAP from upstroke to the time at which repolarization is 90% completed (MAPD<sub>90</sub>). Transmural dispersion of MAPD<sub>90</sub> (TDR) was the difference between endocardial and epicardial MAPD<sub>90</sub>. Triangulation of MAP was the difference of values of MAPD<sub>90</sub> and MAPD<sub>30</sub> of an epicardial MAP.

### Beat-to-beat variability of MAPD<sub>90</sub> (BVR)

Values of epicardial MAPD<sub>90</sub> for 30 consecutive beats were measured, and BVR was determined as the mean orthogonal distance on the Poincaré plot from the diagonal to each point using the following equation:  $\sum |MAPD_{n+1} - MAPD_n| / [30 \times \sqrt{2}]$ .<sup>11</sup>

### Twelve-lead ECG recording

A 12-lead ECG was recorded using a circular Einthoven-Golberger ECG electrode system (Harvard Apparatus Inc., Holliston, MA, USA) connected to a Biopac Wilson ECG amplifier (Biopac, Goleta, CA, USA). Electrophysiologic parameters, including QT and QRS intervals and duration of the T wave from the peak to the end (T<sub>peak</sub>-T<sub>end</sub>), were measured. QT dispersion was the difference between the longest and the shortest QT intervals for a single beat. The ventricular effective refractive period (VERP) was the longest S<sub>1</sub>S<sub>2</sub> interval at which the S<sub>2</sub> stimulus failed to activate the heart when an S<sub>2</sub> stimulus was delivered at increasingly shorter coupling lengths. S<sub>1</sub> stimuli were given at a rate of 1 Hz.

### Determination of proarrhythmic activity of quinidine in the absence and presence of ATX-II

Ectopic ventricular beats, ventricular tachycardia (VT), and early afterdepolarizations (EADs) were monitored continuously and defined as follows: ectopic ventricular beats = spontaneous beats that occurred earlier than the next paced beat; VT or TdP = a sequence of three or more consecutive ectopic ventricular beats at a rate exceeding the pacing rate; and EAD = a positive depolarization during either phase 2 or 3 of a stable MAP signal. Pause-triggered ectopic ventricular beats, EADs, and TdP were those that occurred within the first three beats following a 3-second pause in stimulation and resumption of pacing of the heart.

### Determination of concentration–response relationships for effects of quinidine on electrophysiologic parameters in the absence and presence of ATX-II

Hearts were exposed to increasing concentrations of quinidine (0.1–30 μM) in a cumulative manner, allowing 7 to 15 minutes for each concentration to facilitate recording of a steady-

state effect. To test the effects of quinidine in the presence of ATX-II, hearts were perfused with 1 nmol/L ATX-II for 20 minutes and then exposed to quinidine in the continued presence of ATX-II.

### Effects of quinidine on ion channel currents from rabbit cardiomyocytes—Myocyte isolation

Ventricular myocytes were isolated from female rabbit hearts using an enzymatic method,<sup>12</sup> superfused at a rate of 2 mL/min, and stimulated at a rate of 0.1 Hz. Ion currents were recorded at room temperature (22°–24°C) using a whole-cell patch-clamp technique. Command pulses were generated by a Digidata 1320A controlled by pClamp 8 software (Axon Instruments, Foster City, CA, USA). Series resistance was compensated electronically by 70% to 80%.

For recording of  $I_{Kr}$ , the bath solution (pH 7.4) contained the following (in mmol/L): 132 NaCl, 5 KCl, 1.2 MgCl<sub>2</sub>, 5 HEPES, 5 glucose, and 0.002 nicardipine. The pipette solution (pH 7.2) contained the following (in mmol/L): 119 K-gluconate, 15 KCl, 2.0 MgCl<sub>2</sub>, 5 EGTA, 5 HEPES, and 5 K<sub>2</sub>-ATP. The peak tail current of  $I_{Kr}$  was determined as the amplitude of decaying current immediately following a 250-ms pulse from a holding potential of –50 mV to 10 mV.

For recording of late  $I_{Na}$ , the bath solution contained the following (in mmol/L): 140 NaCl, 5 CsCl, 2.0 MgCl<sub>2</sub>, 1.8 CaCl<sub>2</sub>, 5 HEPES, 5 glucose, and 0.002 nicardipine. The pipette solution contained the following (in mmol/L): 10 NaCl, 130 CsCl, 5 EGTA, 5 HEPES, and 5 ATP-Mg. The amplitude of late  $I_{Na}$  at a voltage of –20 mV was measured at 50 ms after the membrane was depolarized by a 2,000-ms pulse from –140 mV to –20 mV.

For recording of peak  $I_{Na}$ , the bath solution contained the following (in mmol/L): 10 NaCl, 130 CsCl, 1.0 MgCl<sub>2</sub>, 1.0 CaCl<sub>2</sub>, 5 HEPES, 10 glucose, and 0.3 CdCl<sub>2</sub>. The pipette solution contained the following (in mmol/L): 10 NaCl, 110 CsF, 20 CsCl, 5 EGTA, 5 HEPES, and 5 ATP-Mg. Peak  $I_{Na}$  was recorded during an 80-ms duration depolarizing voltage step from –100 to +40. A control current–voltage relationship was obtained, and the amplitude of peak  $I_{Na}$  was measured at a voltage of –30 mV.

### Statistical analysis

All data are reported as mean ± SEM. Concentration–response relationships were analyzed using Prism version 5 (GraphPad Software Inc., San Diego, CA, USA). Repeated measures oneway analysis of variance followed by Newman-Keuls test was used to determine the statistical significance of differences of values before and during drug intervention in the same heart. Paired or unpaired Student's *t*-tests were used to determine the statistical significance of differences between two means before and after drug intervention in the same or different groups. Relative ion currents from single cell were normalized to the respective control (no drug for  $I_{Kr}$  and peak  $I_{Na}$ , and 1 nmol/L ATX-II for late  $I_{Na}$ ).

A generalized linear mixed model with a logit link function was used to determine the probability of an occurrence of TdP for a given increase in the value of a measured electrophysiologic parameter. By treating each heart as a random effect, we investigated the relationship between the occurrence of TdP and each parameter while accounting for differences in responses among hearts. The odds ratio was used to express the change in the relative odds of a TdP event for an increase of 1 SD in the value of a given parameter, and the area under the receiver operating curve (AUROC) was used to summarize the accuracy of each parameter in predicting TdP.<sup>13</sup> An AUROC value of 0.5 indicates that predictive accuracy is no better than chance alone, whereas a value of 1.0 indicates perfect

predictability. Reported AUROC values for common diagnostic tests used in clinical medicine range from 0.52 to 0.95.13

## Results

### Proarrhythmic and antiarrhythmic effects of quinidine in absence and presence of ATX-II

Quinidine at concentrations of 0.3 and 1  $\mu\text{M}$  caused ectopic ventricular beats and spontaneous episodes of TdP in only 1 (7%) and 2 (14%) of 14 female rabbit hearts studied, respectively (Figure 1 and Figure 2B). No ectopic ventricular beats or TdP were observed during exposures to quinidine at concentrations  $\leq 0.1$   $\mu\text{mol/L}$  or 10–30  $\mu\text{mol/L}$ . The proarrhythmic effects of quinidine were greatly enhanced by ATX-II. In the presence of 1 nmol/L ATX-II, quinidine at concentrations of 0.3, 1, and 3  $\mu\text{mol/L}$  caused EADs, ectopic ventricular beats, and spontaneous episodes of TdP in 8 (57%), 13 (93%), and 6 (43%) of 14 hearts (Figure 1 and Figure 2D) studied, respectively ( $P < .001$  vs control). The proarrhythmic effect of quinidine was greatest at concentrations of 0.3–3  $\mu\text{mol/L}$  (Figure 1). Quinidine at concentrations lower than 0.3  $\mu\text{mol/L}$  or greater than 3  $\mu\text{mol/L}$  rarely caused ectopic ventricular beats or TdP in either the absence or presence of ATX-II. In the presence of ATX-II, the maximal number of ectopic ventricular beats per minute was significantly increased by 1  $\mu\text{mol/L}$  quinidine, from  $3 \pm 2$  bpm to  $26 \pm 5$  bpm ( $n = 7$ ,  $P < .01$ ) but decreased to  $0 \pm 0$  bpm when the concentration of quinidine was further increased to 10 and 30  $\mu\text{M}$  (Table 1).

Pauses of 3 to 5 seconds without stimulation are known to be proarrhythmic during exposure of the paced heart to  $I_{K_r}$  blockers. Postpause ectopic ventricular beats and TdP were not observed in hearts treated with either quinidine alone or 1 nmol/L ATX-II alone ( $n = 14$  each, Figures 2G and 2H), whereas pauses during administration of quinidine at concentrations of 0.3, 1, or 3  $\mu\text{mol/L}$  in the presence of 1 nmol/L ATX-II led to ectopic ventricular beats (and TdP) in 3 (21%), 13 (93%), and 7 (50%) of 14 hearts (Figure 1 and Figure 2I). However, in the continued presence of ATX-II, neither ectopic ventricular beats nor TdP were observed when the concentration of quinidine was increased to 10 or 30  $\mu\text{mol/L}$  (Figure 2J).

### Concentration-dependent effects of quinidine on parameters measured from left ventricular MAP and twelve-lead ECG

Quinidine (100 nmol/L to 30  $\mu\text{mol/L}$ ) alone caused a concentration-dependent “monotonic” prolongation of epicardial and endocardial  $\text{MAPD}_{90}$ , triangulation of MAP, and increases of VERP, QT dispersion, and QT and QRS intervals (Figure 3 and Table 1). In contrast, quinidine caused a significant biphasic increase (at concentrations between 0.3 and 3  $\mu\text{M}$ ,  $P < .05$  vs control) and decrease (at concentrations between 10 and 30  $\mu\text{mol/L}$  compared to 1  $\mu\text{mol/L}$ ,  $P < .05$ ) in values of BVR,  $T_{\text{peak-Tend}}$ , and index of  $T_{\text{peak-Tend}}/\text{QT}$  interval (Figure 3 and Table 1).

ATX-II (1 nmol/L) alone caused significant increases ( $P < .05$ –.01) in epicardial and endocardial  $\text{MAPD}_{90}$ , TDR, BVR, triangulation of MAP, QT interval,  $T_{\text{peak-Tend}}$ , index of  $T_{\text{peak-Tend}}/\text{QT}$  interval, QT dispersion, JT interval, and VERP but not in QRS interval ( $P > .05$ ; Figure 3 and Table 1). Quinidine (1  $\mu\text{mol/L}$ ) caused significantly greater increases ( $P < .05$ , Table 1) in epicardial ( $62 \pm 12$  ms vs  $20 \pm 5$  ms,  $n = 10$  and 9;  $P < .01$ ) and endocardial ( $101 \pm 12$  ms vs  $46 \pm 10$  ms,  $n = 10$  and 9;  $P < .01$ )  $\text{MAPD}_{90}$ , TDR ( $39 \pm 12$  ms vs  $27 \pm 6$  ms,  $n = 10$  and 9;  $P < .05$ ), BVR ( $1.23 \pm 0.12$  vs  $0.40 \pm 0.06$ ,  $n = 8$  and 6;  $P < .001$ ), QT interval ( $129 \pm 19$  ms vs  $44 \pm 6$  ms,  $n = 7$  and 8;  $P = .01$ ), JT interval ( $109 \pm 17$  ms vs  $41 \pm 6$  ms,  $n = 7$  and 8;  $P < .05$ ),  $T_{\text{peak-Tend}}$  ( $80 \pm 7$  ms vs  $18 \pm 5$  ms,  $n = 7$  and 8;  $P < .001$ ), and index of  $T_{\text{peak-Tend}}/\text{QT}$  ( $0.12 \pm 0.01$  vs  $0.04 \pm 0.02$ ;  $P < .01$ ) in the presence compared to

the absence of 1 nmol/L ATX-II. Therefore, in the presence of 1 nmol/L ATX-II, the concentration–response relationships for 0.01–1  $\mu$ M quinidine to increase values of the epicardial and endocardial MAPD<sub>90</sub>, BVR, QT interval, JT interval, Tpeak-Tend, and index of Tpeak-Tend/QT interval were left-shifted by 14.6-, 5.8-, 1.5-, 2.0-, 3.3-, 2.2-, and 1.5-fold, respectively (Figure 3 and Table 1). The peak increases in these parameters were associated with EADs, frequent ectopic ventricular beats, and the occurrence of TdP.

When the concentration of quinidine was increased from 1 to 30  $\mu$ mol/L, values of epicardial and endocardial MAPD<sub>90</sub> increased significantly ( $P < .05$  compared to 1  $\mu$ mol/L, Table 1) in the absence but not in the presence of ATX-II. In the presence of ATX-II (1 nmol/L), increasing the quinidine concentration from 1 to 30  $\mu$ mol/L led to significant ( $P < .05$ ) decreases or complete reversal of increases in the values of TDR, BVR, triangulation of MAP, QT interval, Tpeak-Tend, index of Tpeak-Tend/QT, QT dispersion, and JT interval, and further increases ( $P < .05$ ) in VERP and QRS interval (Figure 3 and Table 1). EADs, ectopic ventricular beats, and TdP were not observed in the presence of 10 and 30  $\mu$ mol/L quinidine (Figures 2E and 2J, Table 1). At concentrations of quinidine higher than 30  $\mu$ mol/L in the absence or presence of ATX-II, there was activation failure in hearts paced at a rate of 1 Hz.

Increases in the values of each of seven electrophysiologic parameters were significantly related to increases in the risk of TdP (Table 2 and Figure 4). Based on the magnitude of the AUROC statistic, BVR was the best single predictor of TdP in this study. The AUROC of 0.87 for BVR can be interpreted as the probability that any randomly selected subject with TdP has a BVR value greater than that of any randomly selected subject without TdP. The odds ratio of 5.91 for BVR indicates that an increase in BVR of 1 SD was associated with an increase in the odds of TdP of almost 6-fold. The values of AUROC and the odds ratio for index of Tpeak-Tend/QT interval and Tpeak-Tend were 0.85, 14, 0.83, and 12, respectively.

### Concentration-dependent inhibition by quinidine of I<sub>Kr</sub> and voltage-dependent peak and late I<sub>Na</sub> in rabbit myocytes

Quinidine (1–100  $\mu$ mol/L) caused concentration-dependent inhibitions of I<sub>Kr</sub>, peak I<sub>Na</sub> in the absence of ATX-II, and late I<sub>Na</sub> in the presence of 1 nmol/L ATX-II (Figure 5D). ATX-II (1 nmol/L) significantly increased late I<sub>Na</sub> by 19.6%  $\pm$  1.8%, from 77.1  $\pm$  8.7 pA to 91.8  $\pm$  8.9 pA ( $n = 4$ ,  $P < .01$ ). Representative records of the effects of quinidine on I<sub>Kr</sub>, peak and late I<sub>Na</sub> are shown in Figures 5A through 5C. The estimated IC<sub>50</sub> values for quinidine to reduce I<sub>Kr</sub>, peak I<sub>Na</sub>, and late I<sub>Na</sub> were 4.5  $\pm$  0.3, 11.0  $\pm$  0.7, and 12.0  $\pm$  0.7  $\mu$ mol/L, respectively ( $n = 4$  each). The effect of quinidine on peak I<sub>Na</sub> was voltage dependent (Figure 5C, inset). At a concentration of 1  $\mu$ mol/L, quinidine inhibited I<sub>Kr</sub>, peak I<sub>Na</sub>, and late I<sub>Na</sub> by 22%  $\pm$  2%, 12%  $\pm$  2%, and 10%  $\pm$  1%, respectively (Figure 5D,  $n = 4$  each;  $P < .05$  vs no drug).

## Discussion

Quinidine is used in clinical practice to control atrial and ventricular arrhythmias. Because the drug prolongs VERP and APD and inhibits I<sub>to</sub>, it is increasingly used to treat patients with short QT syndrome or Brugada syndrome.<sup>4–14</sup> However, quinidine itself is a cause of TdP and arrhythmic sudden death. The mechanism of quinidine-induced TdP has been attributed to QT prolongation due to inhibition of I<sub>Kr</sub>.<sup>15,16</sup> The present study examines the critical role of late I<sub>Na</sub> in modulating the arrhythmogenicity of quinidine. Quinidine-induced proarrhythmia was greater at lower (0.3–3  $\mu$ mol/L) than at higher quinidine concentrations, suggesting that inhibition of I<sub>Kr</sub> is alone insufficient to characterize the proarrhythmic potential of the drug. Because low concentrations of quinidine reduce I<sub>Kr</sub> but higher concentrations reduce both I<sub>Kr</sub> and late I<sub>Na</sub>, the proarrhythmia observed with low



concentrations of quinidine in the presence of ATX-II likely reflects a synergistic reduction of net repolarizing current due to concomitant reduction of  $I_{Kr}$  by quinidine and augmentation of late  $I_{Na}$  by ATX-II. That higher concentrations of quinidine were not associated with arrhythmic activity suggests that block of late  $I_{Na}$  by quinidine can balance the effect of  $I_{Kr}$  block to decrease net repolarizing current during phase 3 of the action potential plateau. Thus, the results suggest that the proarrhythmic and antiarrhythmic effects of quinidine are due to reduction and restoration, respectively, of repolarization reserve.

The therapeutic concentration range of quinidine is 3.8 to 10.2  $\mu\text{M}$ .<sup>17</sup> In this study, 0.3–3  $\mu\text{mol/L}$  quinidine was proarrhythmic, whereas 10–30  $\mu\text{mol/L}$  quinidine was not. The values of  $\text{IC}_{50}$  for inhibitions by quinidine of  $I_{Kr}$ , peak  $I_{Na}$ , and late  $I_{Na}$  in rabbit myocytes were  $4.5 \pm 3 \mu\text{mol/L}$ ,  $11.0 \pm 0.7 \mu\text{mol/L}$ , and  $12.0 \pm 0.7 \mu\text{mol/L}$ , respectively (Figure 5). Quinidine previously was reported to inhibit  $I_{Kr}$  with an  $\text{IC}_{50}$  of  $0.4 \pm 0.1 \mu\text{mol/L}$  to  $3.8 \pm 1.2 \mu\text{mol/L}$ .<sup>15</sup> Thus, at a concentration of 1  $\mu\text{mol/L}$ , quinidine is primarily an inhibitor of  $I_{Kr}$ . Even 10% inhibition of  $I_{Kr}$  has been shown to be proarrhythmic when cardiac repolarization reserve is reduced.<sup>9,10</sup> Not surprisingly, in the presence of 1 nmol/L ATX-II, 1  $\mu\text{mol/L}$  quinidine caused a significantly higher incidence of spontaneous or pause-triggered TdP and 1.5- to 14.7-fold greater increases of MAPD, BVR,  $T_{\text{peak-Tend}}$ , QT interval, index of  $T_{\text{peak-Tend}}/\text{QT}$ , and JT interval than in the absence of ATX-II. Higher concentrations (10–30  $\mu\text{mol/L}$ ) of quinidine were not associated with proarrhythmic effects (Figure 1 through Figure 3) because they caused inhibition of  $I_{Na}$ . Similar biphasic proarrhythmic and antiarrhythmic effects have been reported for amiodarone and cisapride, which also are inhibitors of both  $I_{Kr}$  and late  $I_{Na}$ .<sup>9,18</sup>

Basic and clinical research findings indicate that  $I_{Kr}$  inhibitors increase the incidence of TdP in hearts in which late  $I_{Na}$  is enhanced.<sup>9,19,20</sup> Late  $I_{Na}$  can be enhanced by congenital mutations in SCN5A that cause LQTS3, by SCN5A polymorphisms (Y1102 and Y1103), or by acquired cardiac pathologies such as heart failure, myocardial hypertrophy, and ischemia.<sup>21,22</sup> In patients with enhanced late  $I_{Na}$ , an increased proarrhythmic effect of drugs has been reported.<sup>19,20,23</sup> The results in this study suggest that the presence of an enhanced late  $I_{Na}$  may underlie the “idiosyncratic” proarrhythmic effects of quinidine.<sup>1,24</sup>

During repolarization, either a decrease of  $I_{Kr}$  or an increase of late  $I_{Na}$  reduces the net outward current for repolarization of the cardiac action potential (i.e., the repolarization reserve). Quinidine blocks multiple ion channel currents and the inhibitions of  $I_{Kr}$  and  $I_{Na}$  were associated with proarrhythmic and antiarrhythmic electrophysiologic effects, respectively. Thus, a proarrhythmic “window” range of concentrations of quinidine exists wherein there is sufficient block of  $I_{Kr}$  to facilitate the induction of EADs and TdP but insufficient block of late  $I_{Na}$  to act as a counterbalance to maintain repolarization reserve. At concentrations either lower ( $\leq 0.1 \mu\text{M}$ ) or higher ( $\geq 10 \mu\text{M}$ ), inhibition of  $I_{Kr}$  by quinidine either was not enough to be proarrhythmic or was offset by concomitant late  $I_{Na}$  blockade.<sup>25,26</sup>

Inhibition of peak  $I_{Na}$  by quinidine may account for, at least in part, prolongations of QRS interval, ERP,  $\text{MAPD}_{90}$ , and the QT interval, and the occurrence of 1:1 activation failure in hearts exposed to high concentrations ( $\geq 30 \mu\text{M}$ ) of quinidine either in the absence or the presence of ATX-II. An increase in VERP is a rationale for the selection of quinidine to treat patients with short QT syndrome.<sup>4,14</sup>

Many parameters have been used to predict the occurrence of TdP.<sup>9</sup> However, the predictive values of these parameters have not been clarified. In this study, the biphasic increases and decreases of TDR, BVR,  $T_{\text{peak-Tend}}$ , JT interval, and index of  $T_{\text{peak-Tend}}/\text{QT}$  interval in the presence of 1 nM ATX-II were qualitatively correlated with the occurrence of TdP. Both

in the absence and the presence of ATX-II, values of BVR, Tpeak-Tend, and index of Tpeak-Tend/QT interval were significantly increased above either control (quinidine alone) or ATX-II alone by quinidine at a concentration of 1  $\mu\text{M}$  and were associated with the occurrence of TdP. When the concentration of quinidine was increased to 30  $\mu\text{M}$ , TdP did not occur in any heart, and values of BVR, Tpeak-Tend, and index of Tpeak-Tend/QT interval significantly decreased or returned to baseline. Compared to MAPD and QT interval, the parameters BVR, index of Tpeak-Tend/QT interval, and Tpeak-Tend have high predictive accuracy and therefore are better predictors of TdP (Table 2). These results are consistent with previously research studies.<sup>9,27</sup> In contrast, although EADs, ectopic ventricular beats, and episodes of TdP occurred when MAPD and QT interval were prolonged, the relationships between prolongations of MAPD and QT interval and the occurrence of TdP were not as strong as were those for the above-noted parameters (Table 2). The increases of MAPD and QT interval observed in the presence of 10–30  $\mu\text{mol/L}$  quinidine were not associated with TdP, whereas increases in these parameters in the presence of 0.3  $\mu\text{M}$  quinidine were associated with arrhythmia. These results are consistent with clinical observations that quinidine-induced QTc interval prolongation is neither a very sensitive nor a very specific predictor of the proarrhythmic effect of the drug.<sup>28,29</sup>

### Study limitations

In addition to the inhibitions of  $I_{Kr}$ , late  $I_{Na}$ , and peak  $I_{Na}$ , quinidine inhibits  $I_{Ca}$ ,  $I_{Ks}$ ,  $I_{K1}$ , and  $I_{K-ATP}$  at higher concentrations, but the roles of these latter currents were not considered. Monomorphic VT induced by high concentrations of quinidine and programmable ventricular stimulation was not explored. The hearts used in this study were denervated; therefore, quinidine-induced changes in nerve activity and their effect on the occurrence of TdP could not be studied.<sup>30</sup>

### Conclusion

The presence of late  $I_{Na}$  modulates the arrhythmogenicity of quinidine. The proarrhythmic effects of quinidine were significantly greater in the presence than in the absence of ATX-II, suggesting that an increased level of late  $I_{Na}$ , which is associated with a wide variety of pathophysiologic conditions, may lead to an increased incidence of TdP in patients exposed to low or subtherapeutic concentrations of quinidine. Increases of BVR, index of Tpeak-Tend/QT interval, and Tpeak-Tend have higher predictive accuracies than MAPD and QT interval in predicting the occurrence of TdP. The biphasic proarrhythmic and antiarrhythmic effects of low and higher concentrations of quinidine were associated with inhibitions of  $I_{Kr}$  and of  $I_{Na}$  (especially late  $I_{Na}$ ), respectively.

### Acknowledgments

We thank Dr. Whedy Wang for assistance with statistical analysis of experimental data.

Dr. Wu, Hong Li, Dr. Shryock, and Dr. Belardinelli are full-time employees of CV Therapeutics. Dr. Guo, Dr. Yan, and Dr. Jiao receive grant support from CV Therapeutics. Dr. Hackett and Dr. Antzelevitch are consultants for CV Therapeutics.

### References

1. Grace AA, Camm AJ. Quinidine. *N Engl J Med*. 1998; 338:35–45. [PubMed: 9414330]
2. Iost N, Virag L, Varro A, et al. Comparison of the effect of class IA antiarrhythmic drugs on transmembrane potassium currents in rabbit ventricular myocytes. *J Cardiovasc Pharmacol Ther*. 2003; 8:31–41. [PubMed: 12652328]
3. Kaufman ES. Quinidine in short QT syndrome: an old drug for a new disease. *J Cardiovasc Electrophysiol*. 2007; 18:665–666. [PubMed: 17521305]



4. Milberg P, Tegelkamp R, Osada N, et al. Reduction of dispersion of repolarization and prolongation of postrepolarization refractoriness explain the antiarrhythmic effects of quinidine in a model of short QT syndrome. *J Cardiovasc Electrophysiol.* 2007; 18:658–664. [PubMed: 17521304]
5. Marquez MF, Salica G, Hermosillo AG, et al. Ionic basis of pharmacological therapy in Brugada syndrome. *J Cardiovasc Electrophysiol.* 2007; 18:234–240. [PubMed: 17338775]
6. Hermida JS, Denjoy I, Clerc J, et al. Hydroquinidine therapy in Brugada syndrome. *J Am Coll Cardiol.* 2004; 43:1853–1860. [PubMed: 15145111]
7. Roden DM, Woosley RL, Primm RK. Incidence and clinical features of the quinidine-associated long QT syndrome: implications for patient care. *Am Heart J.* 1986; 111:1088–1093. [PubMed: 3716982]
8. Salata JJ, Wasserstrom JA. Effects of quinidine on action potentials and ionic currents in isolated canine ventricular myocytes. *Circ Res.* 1988; 62:324–337. [PubMed: 2448058]
9. Wu L, Rajamani S, Shryock JC, et al. Augmentation of late sodium current unmasks the proarrhythmic effects of amiodarone. *Cardiovasc Res.* 2008; 77:481–488. [PubMed: 18006430]
10. Wu L, Shryock JC, Song Y, et al. An increase in late sodium current potentiates the proarrhythmic activities of low-risk QT-prolonging drugs in female rabbit hearts. *J Pharmacol Exp Ther.* 2006; 316:718–726. [PubMed: 16234410]
11. Thomsen MB, Verduyn SC, Stengl M, et al. Increased short-term variability of repolarization predicts d-sotalol-induced torsades de pointes in dogs. *Circulation.* 2004; 110:2453–2459. [PubMed: 15477402]
12. Rials SJ, Wu Y, Xu X, et al. Regression of left ventricular hypertrophy with captopril restores normal ventricular action potential duration, dispersion of refractoriness, and vulnerability to inducible ventricular fibrillation. *Circulation.* 1997; 96:1330–1336. [PubMed: 9286966]
13. Pepe, M. *The Statistical Evaluation of Medical Tests for Classification and Prediction.* Oxford, UK: Oxford University Press; 2003.
14. Patel C, Antzelevitch C. Cellular basis for arrhythmogenesis in an experimental model of the SQT1 form of the short QT syndrome. *Heart Rhythm.* 2008; 5:585–590. [PubMed: 18362027]
15. Yang T, Roden DM. Extracellular potassium modulation of drug block of  $I_{Kr}$ . Implications for torsade de pointes and reverse use-dependence. *Circulation.* 1996; 93:407–411. [PubMed: 8565156]
16. Roden DM, Anderson ME. Proarrhythmia. *Handb Exp Pharmacol.* 2006; 171:73–97. [PubMed: 16610341]
17. Sokolow M. Some quantitative aspects of treatment with quinidine. *Ann Intern Med.* 1956; 45:582–588. [PubMed: 13363182]
18. Di Diego JM, Belardinelli L, Antzelevitch C. Cisapride-induced transmural dispersion of repolarization and torsade de pointes in the canine left ventricular wedge preparation during epicardial stimulation. *Circulation.* 2003; 108:1027–1033. [PubMed: 12912819]
19. Lehtonen A, Fodstad H, Laitinen-Forsblom P, et al. Further evidence of inherited long QT syndrome gene mutations in antiarrhythmic drug-associated torsades de pointes. *Heart Rhythm.* 2007; 4:603–607. [PubMed: 17467628]
20. Splawski I, Timothy KW, Tateyama M, et al. Variant of SCN5A sodium channel implicated in risk of cardiac arrhythmia. *Science.* 2002; 297:1333–1336. [PubMed: 12193783]
21. Yang P, Kanki H, Drolet B, et al. Allelic variants in long-QT disease genes in patients with drug-associated torsades de pointes. *Circulation.* 2002; 105:1943–1948. [PubMed: 11997281]
22. Belardinelli L, Shryock JC, Wu L, et al. Use of preclinical assays to predict risk of drug-induced torsades de pointes. *Heart Rhythm.* 2005; 2:S16–S22. [PubMed: 16253927]
23. Naccarelli GV, Wolbrette DL, Khan M, et al. Old and new antiarrhythmic drugs for converting and maintaining sinus rhythm in atrial fibrillation: comparative efficacy and results of trials. *Am J Cardiol.* 2003; 91:15D–26D.
24. Reiffel JA. Inpatient versus outpatient antiarrhythmic drug initiation: safety and cost-effectiveness issues. *Curr Opin Cardiol.* 2000; 15:7–11. [PubMed: 10666656]
25. Jackman WM, Friday KJ, Anderson JL, et al. The long QT syndromes: a critical review, new clinical observations and a unifying hypothesis. *Prog Cardiovasc Dis.* 1988; 31:115–172. [PubMed: 3047813]

26. Lazzara R. Antiarrhythmic drugs and torsade de pointes. *Eur Heart J*. 1993; 14 Suppl H:88–92. [PubMed: 8293758]
27. Yamaguchi M, Shimizu M, Ino H, et al. T wave peak-to-end interval and QT dispersion in acquired long QT syndrome: a new index for arrhythmogenicity. *Clin Sci (Lond)*. 2003; 105:671–676. [PubMed: 12857349]
28. Kim SY, Benowitz NL. Poisoning due to class IA antiarrhythmic drugs. Quinidine, procainamide and disopyramide. *Drug Saf*. 1990; 5:393–420. [PubMed: 2285495]
29. Bauman JL, Bauernfeind RA, Hoff JV, et al. Torsade de pointes due to quinidine: observations in 31 patients. *Am Heart J*. 1984; 107:425–430. [PubMed: 6695683]
30. Tan HL, Hou CJ, Lauer MR, et al. Electrophysiologic mechanisms of the long QT interval syndromes and torsade de pointes. *Ann Intern Med*. 1995; 122:701–714. [PubMed: 7702233]

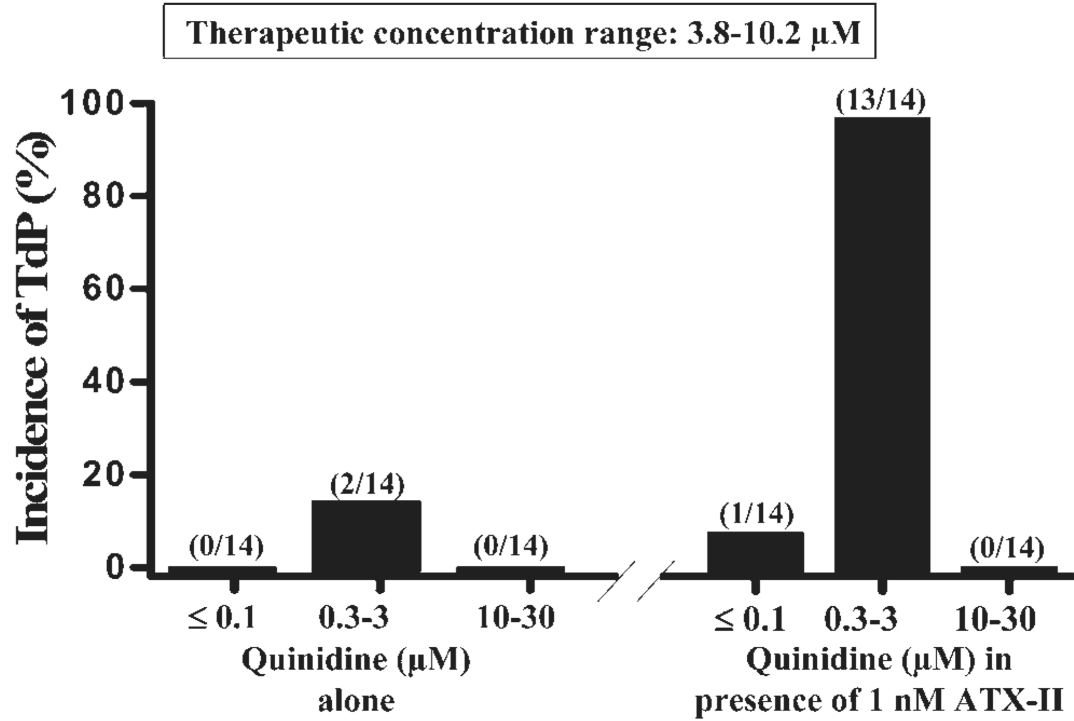


**Figure 1.**

Concentration-dependent biphasic proarrhythmic and antiarrhythmic effects of quinidine in causing torsade de pointes (TdP) in the absence (**left**) and presence (**right**) of 1 nmol/L ATX-II in female rabbit isolated hearts paced at 1 Hz. Numbers in parentheses indicate the number of hearts with TdP and the total number of hearts studied. Therapeutic concentrations range of quinidine is given in the *box* at the top of the figure.

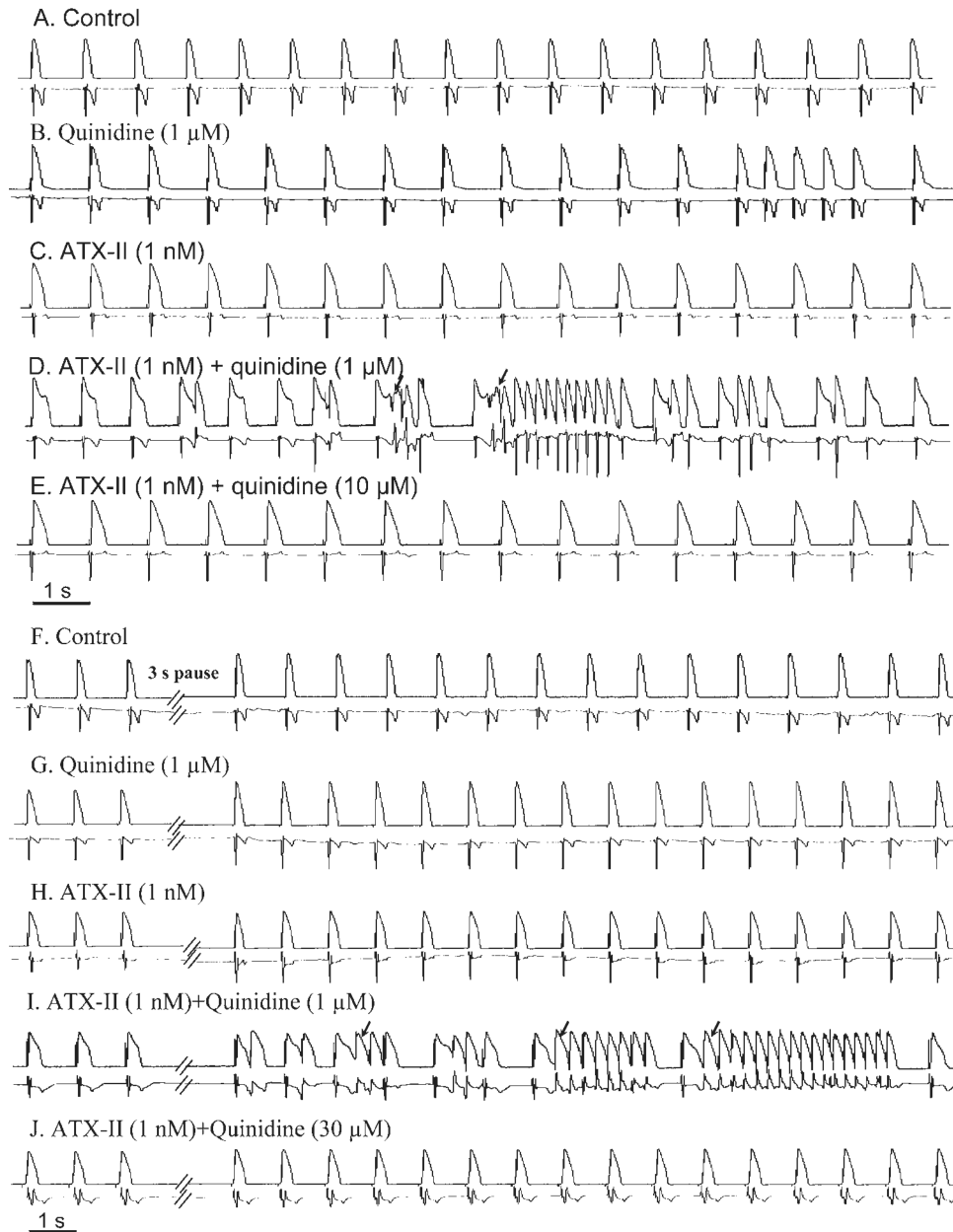


**Figure 2.**

Representative records of concentration-dependent biphasic proarrhythmic and antiarrhythmic effects of quinidine in the presence of 1 nmol/L ATX-II in a female rabbit heart paced at 1 Hz. Monophasic action potentials (top record in each panel) and ECG (bottom record in each panel) were simultaneously recorded. Drug effects recorded during constant pacing at 1 Hz (A–E) and after a 3-second pause (F–J) are shown. Arrows indicate spontaneous or 3-second pause-triggered episodes of torsade de pointes.

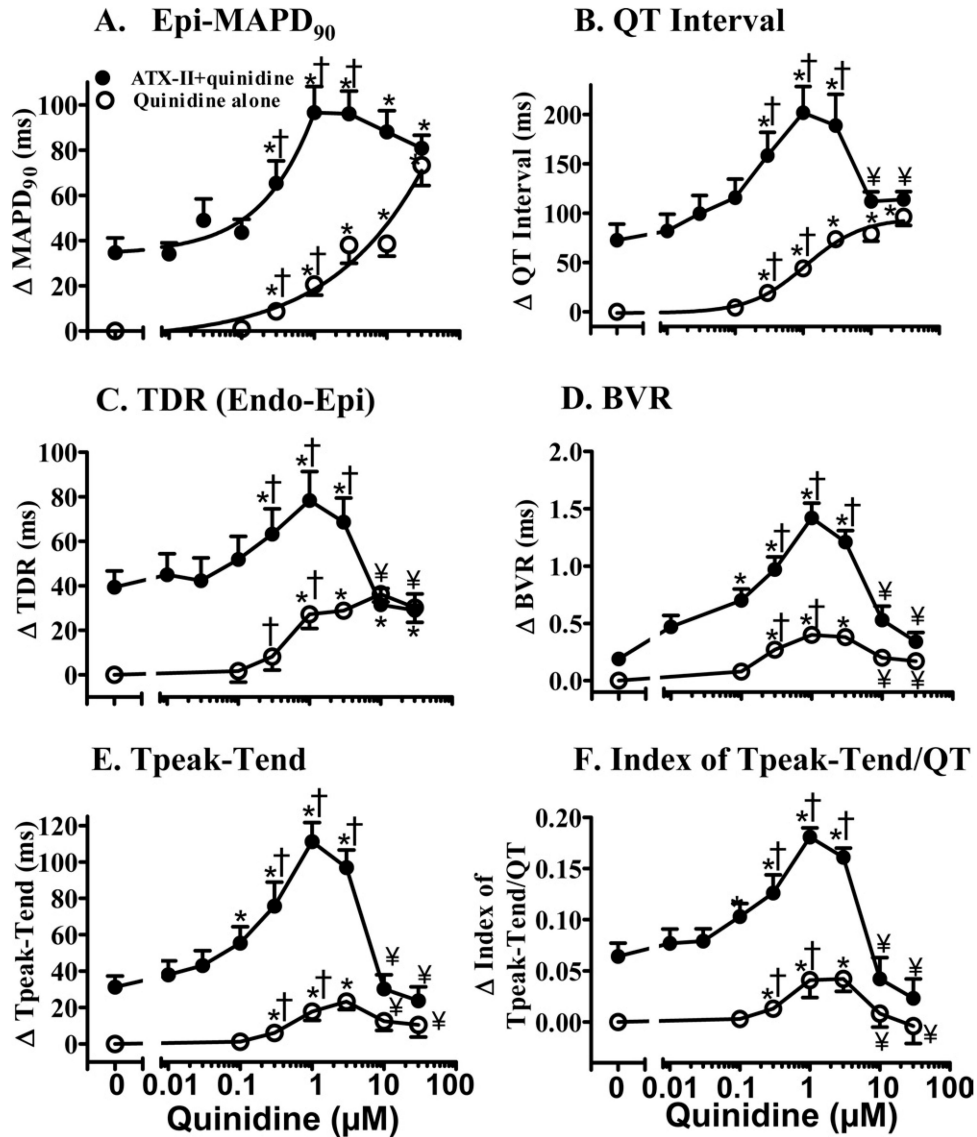


**Figure 3.** Concentration–response relationships for quinidine in increasing epicardial MAPD<sub>90</sub> (A), QT interval (B), transmural dispersion of MAPD<sub>90</sub> (TDR, C), beat-to-beat variability of MAPD<sub>90</sub> (BVR, D), Tpeak-Tend (E), and index of (Tpeak-Tend)/QT interval (F) in the absence (*open symbols*) and the presence (*solid symbols*) of 1 nmol/L ATX-II. Values are calculated as the changes from baseline in each heart and are presented as mean  $\pm$  SEM. Baseline values (control) of these parameters are listed in Table 1 [available as online supplement]. \* $P < .05$  quinidine alone vs control, or ATX-II + quinidine vs ATX-II alone. † $P < .05$  vs ATX-II + 1  $\mu$ mol/L quinidine. ‡TdP occurred at concentrations indicated.

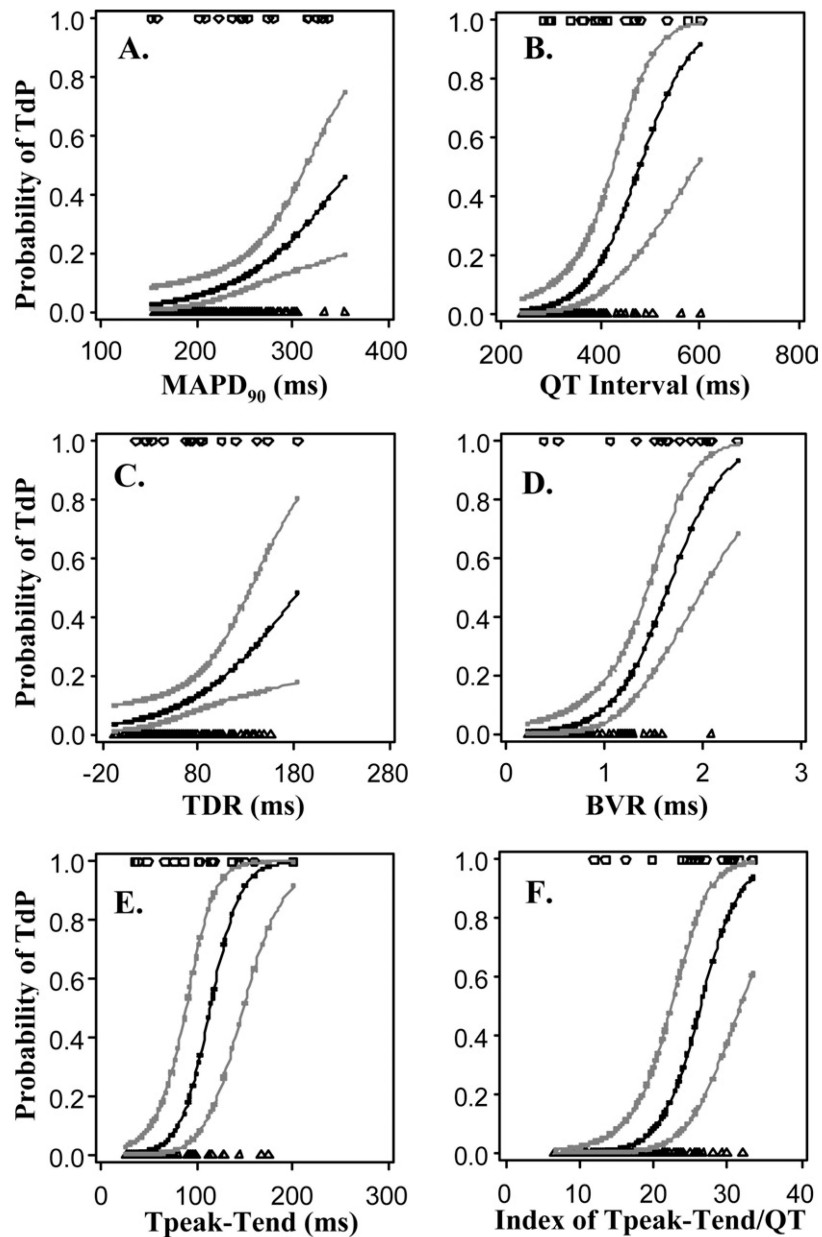


**Figure 4.**

Relationships between an increase in the value of each of six electrophysiologic parameters and the probability of torsade de pointes (TdP) in a female rabbit isolated heart for all tested conditions (control, quinidine, ATX-II + quinidine). Symbols at the top of each plot indicate individual measured values of a given parameter in a heart with TdP (i.e., observed events). Symbols at the bottom of each figure indicate measured values of the same parameter in a heart without TdP (i.e., observed nonevents). Measured values were fitted using a linear mixed model with a logit link function to determine the predicted probability of TdP at any value of the parameter within the range of values recorded experimentally. The 95% confidence intervals for the predicted probabilities are shown. Abbreviations as in Figure 3.



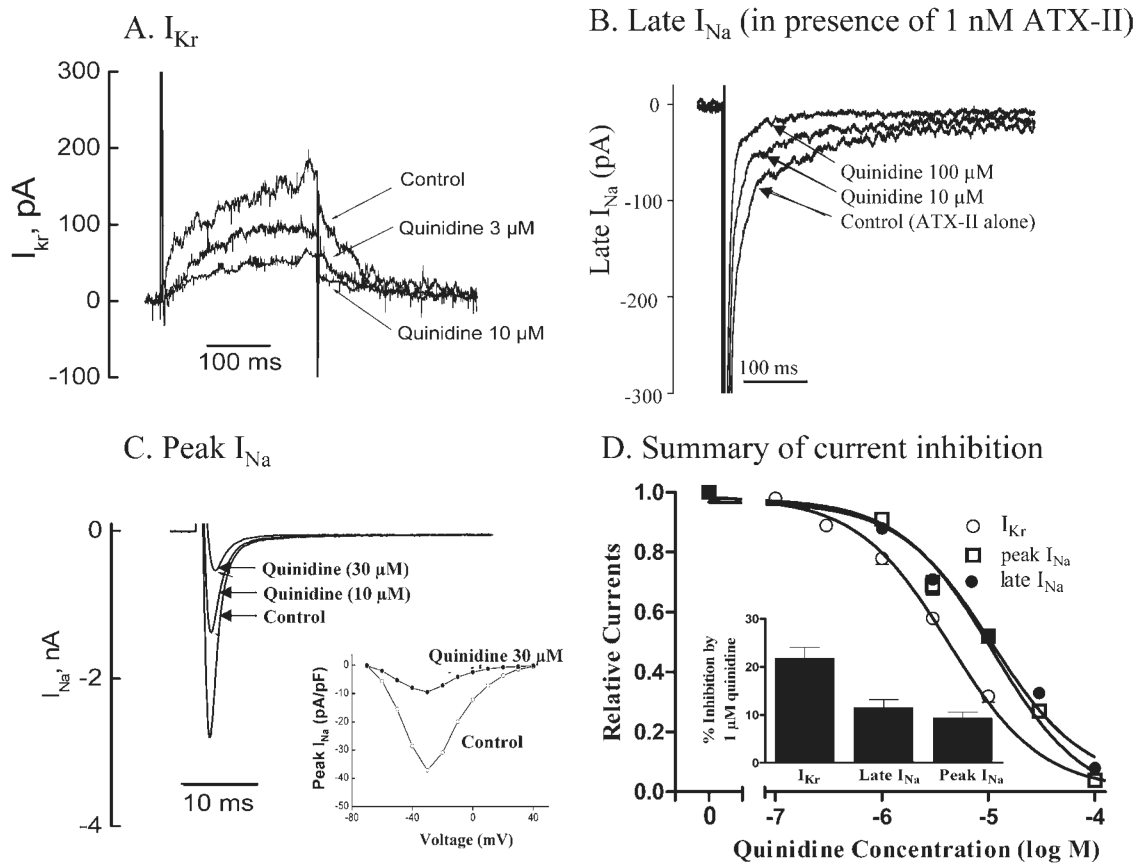


**Figure 5.**

Concentration-dependent inhibitions of  $I_{Kr}$ , late and peak  $I_{Na}$  by quinidine in female rabbit ventricular myocytes. **A:** Representative  $I_{Kr}$  currents from a single cell in the absence of drug (control) and during superfusion with 3 and 10  $\mu\text{mol/L}$  quinidine. **B:** Representative recordings from a single cell of late  $I_{Na}$  in control (1 nmol/L ATX-II alone) and during superfusion with 10 and 100  $\mu\text{mol/L}$  quinidine in the continued presence of 1 nmol/L ATX-II. **C:** Representative recordings of peak  $I_{Na}$  from a single cell in the absence (control) and the presence of 10 and 30  $\mu\text{mol/L}$  quinidine. *Inset* shows current–voltage curves in the absence (*open circles*) and the presence (*solid circles*) of 30  $\mu\text{mol/L}$  quinidine. **D:** Summarized concentration–response relationships for inhibitions of  $I_{Kr}$ , peak and late  $I_{Na}$  by quinidine ( $n = 4$  for each).

Table 1

Effect of quinidine on electrophysiologic parameters in absence and presence of 1 nmol/L ATX-II

Electrophysiologic parameter	Quinidine alone ( $\mu\text{M}$ )			ATX-II (1 nM) + Quinidine ( $\mu\text{M}$ )		
	0	1	30	0	1	30
Epi-MAPD <sub>90</sub>	181 $\pm$ 4 (n = 20)	194 $\pm$ 7 (n = 9) <sup>*</sup>	248 $\pm$ 10 (n = 8) <sup>***††</sup>	220 $\pm$ 9 (n = 10) <sup>***</sup>	282 $\pm$ 14 (n = 10) <sup>††</sup>	267 $\pm$ 7 (n = 10) <sup>††</sup>
Endo-MAPD <sub>90</sub>	202 $\pm$ 4 (n = 20)	240 $\pm$ 9 (n = 9) <sup>**</sup>	298 $\pm$ 5 (n = 8) <sup>***††</sup>	283 $\pm$ 13 (n = 10) <sup>***</sup>	384 $\pm$ 20 (n = 10) <sup>††</sup>	319 $\pm$ 10 (n = 10) <sup>††</sup>
TDR	21 $\pm$ 2 (n = 20)	46 $\pm$ 7 (n = 9) <sup>**</sup>	50 $\pm$ 7 (n = 8) <sup>**</sup>	63 $\pm$ 8 (n = 10) <sup>**</sup>	102 $\pm$ 15 (n = 10) <sup>††</sup>	52 $\pm$ 8 (n = 10) <sup>†</sup>
BVR	0.36 $\pm$ 0.02 (n = 13)	0.73 $\pm$ 0.05 (n = 6) <sup>***††</sup>	0.50 $\pm$ 0.06 (n = 6) <sup>***††</sup>	0.57 $\pm$ 0.03 (n = 8) <sup>**</sup>	1.81 $\pm$ 0.12 (n = 8) <sup>††</sup>	0.72 $\pm$ 0.07 (n = 8) <sup>††</sup>
Triangulation	84 $\pm$ 3 (n = 20)	103 $\pm$ 7 (n = 9)	124 $\pm$ 18 (n = 8) <sup>*</sup>	117 $\pm$ 8 (n = 9) <sup>**</sup>	157 $\pm$ 11 (n = 9) <sup>††</sup>	117 $\pm$ 5 (n = 9) <sup>†</sup>
QT Interval	265 $\pm$ 5 (n = 14)	317 $\pm$ 8 (n = 8) <sup>**</sup>	369 $\pm$ 10 (n = 8) <sup>***††</sup>	340 $\pm$ 21 (n = 7) <sup>***</sup>	469 $\pm$ 31 (n = 7) <sup>††</sup>	381 $\pm$ 9 (n = 7) <sup>†</sup>
Tpeak-Tend	32 $\pm$ 2 (n = 14)	55 $\pm$ 5 (n = 8) <sup>*</sup>	42 $\pm$ 6 (n = 8) <sup>***†</sup>	65 $\pm$ 6 (n = 7) <sup>**</sup>	145 $\pm$ 11 (n = 7) <sup>††</sup>	58 $\pm$ 7 (n = 7) <sup>††</sup>
Tpeak-Tend/QT	0.12 $\pm$ 0.01 (n = 14)	0.16 $\pm$ 0.02 (n = 8) <sup>*</sup>	0.11 $\pm$ 0.02 (n = 8) <sup>†</sup>	0.19 $\pm$ 0.01 (n = 7) <sup>**</sup>	0.31 $\pm$ 0.01 (n = 7) <sup>††</sup>	0.15 $\pm$ 0.02 (n = 7) <sup>†††</sup>
QT dispersion	15 $\pm$ 2 (n = 11)	38 $\pm$ 4 (n = 7) <sup>**</sup>	45 $\pm$ 7 (n = 7) <sup>**</sup>	29 $\pm$ 4 (n = 6) <sup>**</sup>	76 $\pm$ 13 (n = 6) <sup>††</sup>	29 $\pm$ 4 (n = 6) <sup>†</sup>
JT interval	189 $\pm$ 7 (n = 14)	242 $\pm$ 6 (n = 8) <sup>***</sup>	252 $\pm$ 6 (n = 8) <sup>***†</sup>	259 $\pm$ 26 (n = 6) <sup>***</sup>	370 $\pm$ 32 (n = 7) <sup>††</sup>	264 $\pm$ 10 (n = 7) <sup>†††</sup>
VERP	160 $\pm$ 6 (n = 12)	191 $\pm$ 13 (n = 7) <sup>**</sup>	279 $\pm$ 6 (n = 7) <sup>***††</sup>	168 $\pm$ 6 (n = 5) <sup>*</sup>	198 $\pm$ 5 (n = 5) <sup>††</sup>	314 $\pm$ 5 (n = 5) <sup>††††</sup>
QRS interval	77 $\pm$ 2 (n = 14)	76 $\pm$ 3 (n = 8)	127 $\pm$ 7 (n = 8) <sup>***††</sup>	82 $\pm$ 2 (n = 7)	87 $\pm$ 2 (n = 7) <sup>†</sup>	143 $\pm$ 5 (n = 7) <sup>††††</sup>
EVBs	0 $\pm$ 0 (n = 15)	1 $\pm$ 1 (n = 8)	0 $\pm$ 0 (n = 8)	5 $\pm$ 2 (n = 7)	18 $\pm$ 2 (n = 7) <sup>††</sup>	0 $\pm$ 0 (n = 7) <sup>††</sup>

Summary of electrophysiologic measures in the absence of drug (control) and the presence of either quinidine alone (1 and 30  $\mu\text{mol/L}$ ) or ATX-II (1 nmol/L) + quinidine.Underlined numbers indicate that changes in the given parameter were maximal at a concentration of 3  $\mu\text{mol/L}$ .BVR = beat-to-beat variability of MAPD<sub>90</sub>; EVB = ectopic ventricular beat; monophasic action potential duration from upstroke to the time at which repolarization is 90% completed; TDR = transmural dispersion of MAPD<sub>90</sub>; VERP = ventricular effective refractory period.\*  $P < .05$  or  $P < .01$  vs control, 1 nmol/L ATX-II, and 1 nmol/L ATX-II + 1  $\mu\text{mol/L}$  quinidine, respectively.

**Table 2**

Summary of relationships between electrophysiologic parameters and occurrence of torsade de pointes in isolated rabbit heart under control, quinidine, and quinidine plus ATX-II conditions

Electrophysiologic parameter	P value*	Odds ratio <sup>†</sup>		AUROC‡
		Estimate	95% Confidence interval	
MAPD <sub>90</sub>	.0029	2.21	(1.32, 3.72)	0.69
QT interval	<.0001	4.16	(2.05, 8.41)	0.74
TDR	.0074	1.86	(1.18, 2.29)	0.68
BVR	<.0001	5.91	(2.71, 12.89)	0.87
Tpeak-Tend	<.0001	11.82	(4.52, 30.95)	0.83
Index of Tpeak-Tend/QT	<.0001	14.29	(4.90, 41.65)	0.85
JT interval	<.0001	4.85	(2.28, 10.32)	0.74

AUROC = area under the receiver operating curve; BVR = beat-to-beat variability of MAPD<sub>90</sub>; CI = confidence interval; MAPD<sub>90</sub> = monophasic action potential duration from upstroke to the time at which repolarization is 90% completed; TDR = transmural dispersion of MAPD (difference between endocardial and epicardial MAPD<sub>90</sub>).

\* Significance of the relationship between the increase of the value of a given electrophysiologic parameter and the occurrence of torsade de pointes.

<sup>†</sup> For an increase equivalent to 1 SD in the value of a given parameter.

<sup>‡</sup> Larger values indicate greater accuracy in predicting torsade de pointes.

<sup>‡</sup> Larger values indicate greater accuracy in predicting torsade de pointes.